Energy Equip. Sys./ Vol. 5/No . 3/September 2017/ 299-312

ENERGY EQUIPSYS

Energy Equipment and Systems

http://energyequipsys.ut.ac.ir
www.energyequipsys.com

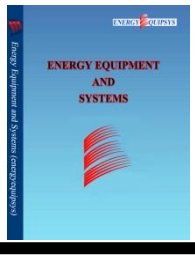

The energy and exergy analysis of a novel cogeneration organic Rankine power and two-stage compression refrigeration cycle

Authors

Hamed Mortazavi Beni [a]
Afshin Ahmadi Nadooshan [a*]
Morteza Bayareh [a]

[a] Department of Mechanical Engineering, Shahrekord University, Shahrekord,Iran

Article history:

Received : 13 February 2017
Accepted : 24 April 2017

ABSTRACT

The energy crisis in recent years has led to the use of thermodynamic cycles that work based on renewable energies. Low-temperature cycles—such as organic cycles—are suitable strategies for the application of renewable energies. The present study proposes a novel cycle through the integration of a two-stage compression refrigeration cycle with a combined Rankine power and ejector refrigeration cycle by using the cascade condenser method. The fundamental idea of this cycle is to obtain refrigeration production at lower temperatures, and to achieve higher thermal and exergy efficiencies. The results showed that the new cycle recorded an 11.67 percent improvement in thermal efficiency and a 16.89 percent improvement in exergy efficiency compared to the basic cycle. Even though the network output of the cycle is reduced, a significant increase in the refrigeration capacity of the cycle is observed.

Keywords: Cogeneration Cycle, Exergy, Solar Energy, Ejector, Cascade Condenser.

1. Introduction

In this research, the new cogeneration organic Rankine power and two-stage compression refrigeration cycle has been analyzed from the viewpoint of energy and exergy. In this cycle, solar energy is used as the heat source. Nowadays, solar energy is considered more frequently because it is a clean and renewable energy. While the use of solar collectors and setting up the cycles with solar energy as the heat source has higher initial costs, the current cycle cost is much lower due to the lack of environmental costs and as fossil fuels are not required. This issue is also significant with regard to the lack of environmental pollution in the solar cycles. Low-temperature cycles—such as cycles that use organic fluids as refrigerants—are the proper approach for using sustainable, clean, and renewable energies such as geothermal and solar energy. Zhang et al. [1] evaluated the performance of the double-compression flash intercooling refrigeration cycle in comparison with the double-compression external intercooling cycle. The results showed that the double-compression flash intercooling refrigeration cycle and the double-compression external intercooling cycle yield the maximum coefficient of performance improvement of 23.18% and 11.03% over the basic cycle, respectively. There are numerous methods for improving the performance of the vapor-compression refrigeration cycle. One of these methods involves the use of an ejector as an expander device. Using an ejector is preferred due to the high efficiency and the lack of mechanical rotary components, which reduces depreciation. Nowadays, the ejector

*Corresponding author: Afshin Ahmadi Nadooshan
Address: Department of Mechanical Engineering, Shahrekord University, Shahrekord,Iran
E-mail address: ahmadi@eng.sku.ac.ir

is used in many mechanical cycles such as power plants and compression refrigeration cycles. So far, many research studies have focused on ejector expansion compression refrigeration cycles [2–6]. In this research, the ejector is used as an expander device in the compression refrigeration cycle instead of using an expansion valve in order to avoid the work and energy losses in the expansion valve. In another study, Xing et al. [7] proposed an ejector subcooled vapor-compression refrigeration cycle. The results showed that the performance of the ejector subcooled cycle is better than that of the conventional cycle. Wang et al. [8] compared the use of the ejector expander in the vapor-compression refrigeration cycles for applications in domestic refrigerator freezers and presented a novel modified ejector expansion vapor-compression refrigeration cycle. Zhu and Jiang [9] developed a refrigeration system by combining the basic vapor-compression refrigeration cycle with an ejector cooling cycle. In this system, the ejector-cooling cycle is driven by the waste heat from the condenser in the vapor-compression refrigeration cycle. The results show that the coefficient of performance is improved by 9.1% in the hybrid refrigeration system. The ejector application domain is not limited to the vapor-compression refrigeration cycle. It is used in many cases, such as in the petroleum and petrochemical industries for the purification and separation of crude oil, and also as a vacuum pump in devices such as condensers. The ejector is also used in the ejector refrigeration cycle. So far, many researches on ejector refrigeration cycles, as well as on combined Rankine power and ejector refrigeration cycles, have been carried out. Chen et al. [10] studied the interactions and relationships of various ejector parameters in the ejector refrigeration system to gain access to an optimum generator temperature that obtains the maximum Carnot efficiency. Sorouradin et al. [11] investigated the performance of an ejector refrigeration cycle theoretically and experimentally. The results indicate a decrease in the coefficient of performance with increasing generator temperature and an increase in the second law of efficiency with increasing evaporator temperature and decreasing generator temperature. Adrian et al. [12] optimized an ejector refrigeration system with different working fluids that operates on waste heat provided by the exhausted gas of an internal combustion engine by energy and exergy analysis. Lontsi et al. [13] proposed a multi-temperature compression–ejection refrigeration cycle by combining a compression refrigeration cycle and an ejector refrigeration cycle. They suggested using this multi-temperature refrigeration cycle instead of the conventional two-stage vapor-compression refrigeration system. By adding a steam turbine before the ejector in ejector refrigeration, the new cycle can be based on combined power generation and ejector refrigeration. Many research studies have focused on such cycles [14–18]. In these researches, the researchers investigated the factors affecting the cycle, such as the input and output temperature, the pressure of the turbine, the evaporator temperature, and the entrainment ratio of the ejector to analyze and optimize the combined Rankine power and ejector refrigeration cycle. In other researches, Yang et al. [19–20] analyzed the combined power and refrigeration cycle by using a zeotropic refrigerant with different mixture compositions. The result showed that using a 50/50 composition of isobutane/pentane has the maximum exergy efficiency of 7.83%. In another study, Yang et al. [21] proposed a novel combined power and ejector-refrigeration cycle by using the two-stage condensation of a zeotropic mixture. Also, a zeotropic mixture is divided into the power cycle and the ejector refrigeration cycle in different compositions. The result revealed that the cycle exergy efficiency achieves a maximum value of 10.29% with the use of a 40/60 percent composition of isobutane/pentane, and the thermal efficiency yields a maximum value of 10.77% with the use of a 70/30 percent composition of an isobutane/pentane zeotropic mixture.

In the current study, the novel cycle is proposed by the integration of a two-stage compression refrigeration cycle with a combined Rankine power and ejector refrigeration cycle by using the cascade condenser method. Since the ejector refrigeration cycle cannot produce refrigeration at very low temperatures, the fundamental idea of this cycle is based on further refrigeration production at lower temperatures by using the solar energy results in higher thermal and exergy efficiencies.

Nomenclature

$\dot{m}$	mass flow rate (kgs^{-1})
h	enthalpy ($kJkg^{-1}$)

$\dot{W}$	work rate (kW)
$\dot{E}x$	flow exergy rate (kW)
$\dot{Q}$	heat transfer rate (kW)
$\dot{I}$	exergy destruction (kW)
T	temperature (^{o}C)
u	velocity (m/s)
s	entropy ($kJkg^{-1}K^{-1}$)
P	pressure (kPa)

Greek Symbols

η_{ex}	exergy efficiency
η_{th}	thermal efficiency
η_{is}	isentropic efficiency
μ	entrainment ratio

Subscripts

0	ambient conditions
i	inlet
e	outlet
o	out
s	surface
des	exergy destruction
L	cooled environment
evap	evaporator
comp	compressor
cond	condenser
expan	expansion valve
Cas.Cond	cascade condenser
Se	separator
is	isentropic
T	turbine
B	boiler
P	pump
C1	Compressor 1
C2	Compressor 2
n	primary nozzle
m	mixing chamber
d	diffuser
w	water

2. Cycle description

The proposed cogeneration Rankine power and two-stage compression refrigeration cycle consists of a combined Rankine power and ejector refrigeration cycle and the two-stage compression refrigeration cycle. First, the refrigerant fluid, by taking heat in the steam generator through the solar collector, and by increasing in temperature and pressure, changes into superheated steam. Usually from water or industrial oils used as primary fluid through the solar collector absorber. In this study, primary fluid from the industrial oil Therminol 66 is used in the absorbent collector. Therminol 66 is the world's most popular high-temperature, liquid-phase heat-transfer fluid. Therminol 66 is pumpable at low temperatures and offers thermal stability at high temperatures. This oil is used in a wide variety of systems, such as the production of plastics and polymers, refining, synthetic fiber manufacturing, chemical processing, water purification, solar collectors, and organic Rankine cycle applications. Since this oil has good stability even at the highest recommended temperature for oil in continuous use in the system, it also has considerable resistance against fouling. Fouling tends to reduce system efficiency and increase costs. Hence, this oil is suggested for use in solar cycles. Using Therminol 66 as the primary fluid in the solar collectors can easily provide superheated vapor in the generator from the working fluid of the organic Rankine cycle even at temperatures up to 300°C. The superheated vapor expands through the turbine to produce power. The turbine output that is still superheated vapor is used as the primary flow in the ejector. The inlet high-pressure primary fluid of the ejector passes through the converging–diverging nozzle. Then, by a vertical shock wave, the pressure energy of the fluid is converted to kinetic energy and the fluid velocity becomes supersonic. The result of this process creates a low-pressure area and produces the high-vacuum area at the inlet of the ejector secondary fluid that entrains the secondary fluid into the mixing chamber of the ejector. So, the suction of the secondary fluid creates the required pressure drop in the evaporator to evaporate the refrigerant and produce a refrigeration effect. After mixing the primary and secondary flow in the mixing chamber through the constant diameter throat of the ejector, the fluid undergoes another shock wave; finally, the pressure of the fluid increases through the divergent diffuser of the ejector. The ejector outlet pressure is between the pressure of the primary and secondary flows. In the following step, the refrigerant fluid condensates through the first condenser. Then, to complete the processing part, the fluid is pumped into the vapor generator, and the rest of the refrigerant fluid passes through the expansion valve and is driven to the

evaporator. The cogeneration Rankine power and two-stage compression refrigeration cycle in this study is started up and operated by solar energy. Figure 1 shows a schematic diagram of the discussed cycle.

The process from the evaporator of the combined power and the ejector refrigeration cycle used as the cascade condenser to the primary condensing of the vapor refrigerant in the two-stage compression refrigeration cycle is shown in Fig. 3. Here, the refrigerant of the two-stage vapor-compression refrigeration cycle passes through Compressor 1 and increases the pressure driven to the cascade condenser where the primary condensate lies. The cascade condenser output that is still in the two-phase mixture of the refrigerant is entered into the vapor–liquid separator. Then, the cascade condenser output mixed with Flow 16 in the separation and the final composition is the two-phase mixture of the refrigerant. The saturated vapor refrigerant moves to Compressor 2 for high-pressure compression. Then, the secondary condensate in Condenser 2 transforms to the saturated liquid state and after passing through the expansion valve returns again to the separator. Also, the saturated liquid part of the refrigerant mixture in the separator moves into Expansion Valve 3. It is then driven to the evaporator for refrigeration production and completion of the cycle. The use of the two-stage compression technique not only helps to reduce the power consumption of the compressors but also, because of the two-stage condensation and expansion processes, allows the cycle to produce more refrigeration at lower temperatures. The following assumptions are made for the simulation of the cycle:

1) All cycle processes are steady-state, steady-flow processes, and the effects of kinetic and potential energy are neglected. The pressure drop and heat losses in the pipes and system components are negligible.
2) The condensers and the evaporator outlet state are the intended saturated liquid and saturated vapor, respectively. The condenser-saturated temperature is considered to be 20°C; according to the source [14], the ambient temperature and pressure are assumed to be 15°C and 101.35 kPa, respectively.
3) The condensers heat exchangers are considered water cooling and the evaporator heat exchanger is considered air cooling.
4) The flow across the expansion valves is isenthalpic.
5) The ejector flow is steady-state and one-dimensional. The velocity of streams at the inlet and outlet of the ejector is negligible.
6) For simplicity, the effects of the stream losses in the frictional and mixing processes in the nozzle, mixing, and diffuser sections are considered to be the isentropic efficiency of the nozzle, the mixing chamber, and the diffuser. Also, the ejector processes are assumed to be adiabatic and do not exchange heat with the environment.
7) Since in comparing the primary flow velocity, the secondary flow velocity is negligible, it is assumed that the suction process is ideal and without a pressure drop.

Therefore, the mixing process in the mixing chamber of the ejector occurs at the suction pressure. It complies with the laws of conservation of energy and momentum.

3.Simulation

The equations governing on the cycle are conservation of the mass, energy and exergy. In discussed cycle we are dealing with flow exergy and steady state steady flow processes. The conservation of mass, energy and exergy are expressed as follows:

$$\sum \dot{m}_i = \sum \dot{m}_e \tag{1}$$

$$\sum \dot{m}_i h_i + \dot{Q} = \sum \dot{m}_e h_e + \dot{W} \tag{2}$$

$$\dot{I} = \sum \dot{E} x_i - \sum \dot{E} x_e + \sum \left(1 - \frac{T_0}{T_s}\right) \dot{Q}_s - \dot{W} \tag{3}$$

In these equations, h denotes enthalpy, $\dot{Q}$ is the heat transfer rate, $\dot{W}$ is work, and $\dot{I}$ is irreversibility or exergy destruction. In the conservation of exergy, $\left(1 - \frac{T_0}{T_S}\right) \dot{Q}_S$ refers to the heat transfer exergy. The heat transfer of the control surface is the maximum obtainable work from the transferred thermal energy $\dot{Q}_S$ at temperature T_S. This term of the exergy balance equation will apply only on devices that involve heat transfer with the environment (heat exchanger), such as in an air-cooled evaporator. In the adiabatic

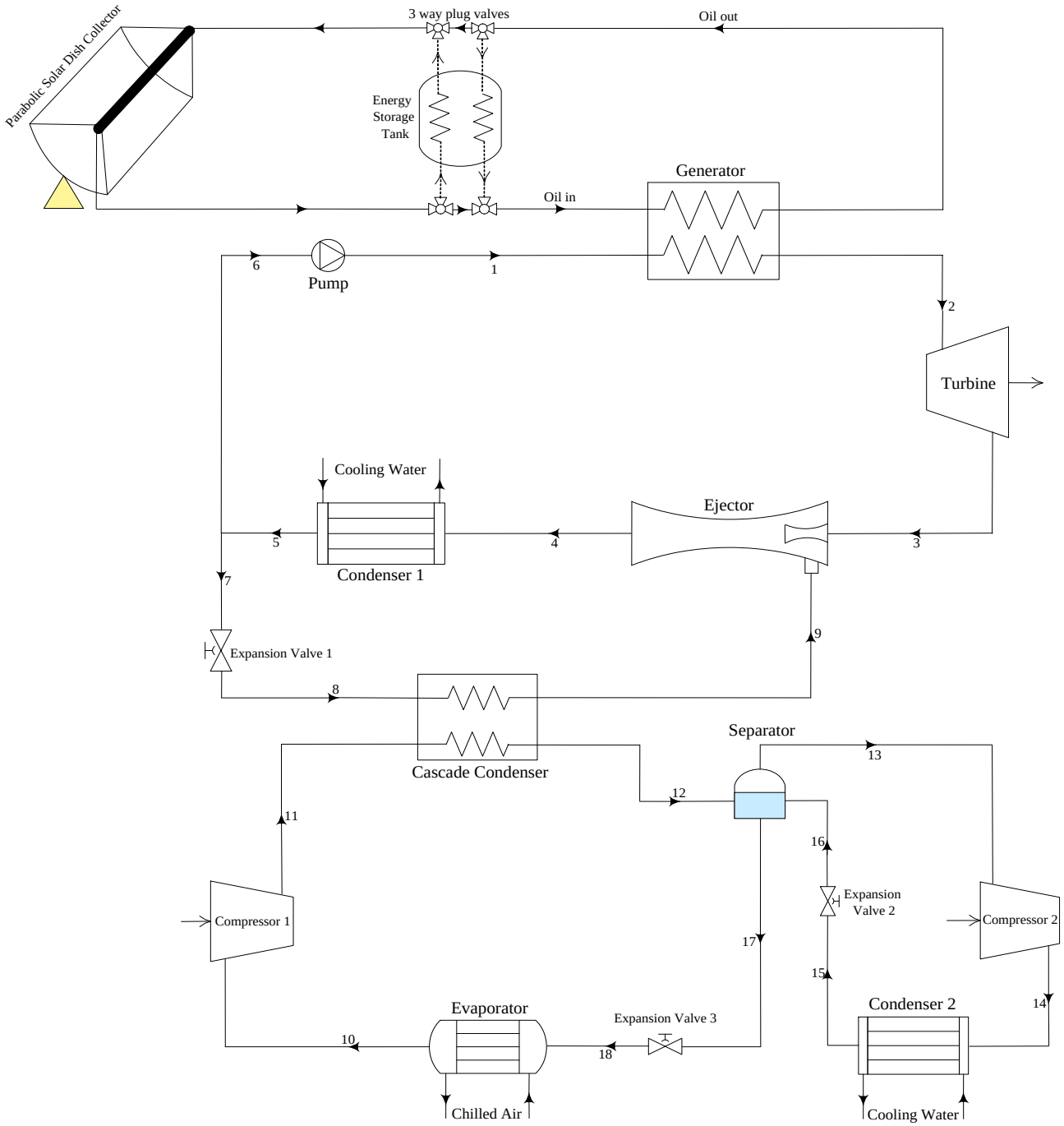

Fig 1. Schematic diagram of cogeneration rankine power and two stage compression refrigeration cycle

processes, where the heat transfer rate is considered to be zero, such as in compressors, this term of the exergy balance equation will be removed. By taking the control volume for every single component of the thermal cycle and applying the conservation of mass, energy, and exergy for the various components of the cycle, the equations for the exergy and energy analysis, and the calculation of the exergy destruction of the cycle components can be achieved. According to Fig. 1, these equations are defined in Table 1 by using Eqs. (1) to (3). $\dot{E}x$ is the thermo-physical exergy flow rates of streams, given as:

$$\dot{E}x = \dot{m}(h - h_0 - \mathrm{T}_0(s - s_0)) \tag{4}$$

The isentropic efficiency of the compressors can be defined as a function of the compressor pressure ratio [23]. The isentropic efficiency of the compressors can be expressed as:

$$\eta_{is} = 0.874 - 0.0135\frac{P_o}{P_i} \tag{5}$$

where $\mathrm{P_i}$ and $\mathrm{P_o}$ are the compressor suction and discharge pressures, respectively.

Table 1. Energy and exergy destruction equations for the various components of the combined cycle

Components	Energy balance	Exergy destruction
Boiler	$\dot{m}_{oil}\cdot\left(h_{oil,i}-h_{oil,o}\right)=\dot{m}_1\cdot\left(h_2-h_1\right)$	$\dot{I}_B=\dot{E}x_{oil,i}+\dot{E}x_1-\dot{E}x_{oil,o}-\dot{E}x_2$
Turbine	$W_T=\eta_{T,s}.\dot{m}_2\cdot\left(h_2-h_{3,s}\right)$	$\dot{I}_T=\dot{E}x_2-\dot{E}x_3-\dot{W}_T$
Pump	$W_P=\dot{m}_6\dfrac{h_{1,s}-h_5}{\eta_{P,s}}$	$\dot{I}_P=\dot{E}x_6-\dot{E}x_1+\dot{W}_P$
Ejector	$\dot{m}_3h_3+\dot{m}_9h_9=\dot{m}_4h_4$	$\dot{I}_{Ej}=\dot{E}x_3+\dot{E}x_9-\dot{E}x_4$
Condenser 1	$\dot{Q}_{cond1}=\dot{m}_5\cdot\left(h_4-h_5\right)$	$\dot{I}_{cond1}=\dot{E}x_4+\dot{E}x_{w,i,c1}-\dot{E}x_5-\dot{E}x_{w,o,c1}$
Condenser 2	$\dot{Q}_{cond2}=\dot{m}_{15}\cdot\left(h_{14}-h_{15}\right)$	$\dot{I}_{cond2}=\dot{E}x_{14}+\dot{E}x_{w,i,c2}-\dot{E}x_{15}-\dot{E}x_{w,o,c2}$
Cascade condenser	$\dot{m}_9\cdot\left(h_9-h_8\right)=\dot{m}_{11}\cdot\left(h_{11}-h_{12}\right)$	$\dot{I}_{CaCo}=\dot{E}x_8+\dot{E}x_{11}-\dot{E}x_9-\dot{E}x_{12}$
Evaporator	$\dot{Q}_{evap}=\dot{m}_{18}\cdot\left(h_{10}-h_{18}\right)$	$\dot{I}_{evap}=\dot{E}x_{19}-\dot{E}x_{10}+\dot{Q}_{evap}(1-\dfrac{T_0}{T_L})$
Separator	$\dot{m}_{12}h_{12}+\dot{m}_{16}h_{16}=\dot{m}_{12}h_{17}+\dot{m}_{16}h_{13}$	$\dot{I}_{Se}=\dot{E}x_{12}+\dot{E}x_{16}-\dot{E}x_{13}-\dot{E}x_{17}$
Expansion valve 1	$h_8=h_7$	$\dot{I}_{expan1}=\dot{E}x_7-\dot{E}x_8$
Expansion valve 2	$h_{16}=h_{15}$	$\dot{I}_{expan2}=\dot{E}x_{15}-\dot{E}x_{16}$
Expansion valve 3	$h_{18}=h_{17}$	$\dot{I}_{expan3}=\dot{E}x_{17}-\dot{E}x_{18}$
Compressor 1	$W_{C1}=\dot{m}_{10}\dfrac{h_{11,s}-h_{10}}{\eta_{C1,s}}$	$\dot{I}_{C1}=\dot{E}x_{10}+\dot{W}_{C1}-\dot{E}x_{11}$
Compressor 2	$W_{C2}=\dot{m}_{13}\dfrac{h_{14,s}-h_{13}}{\eta_{C2,s}}$	$\dot{I}_{C2}=\dot{E}x_{13}+\dot{W}_{C2}-\dot{E}x_{14}$

The thermal efficiency of the cogeneration Rankine power and two-stage compression refrigeration cycle is expressed as:

$$\eta_{th}=\frac{\dot{W}_{net}+\dot{Q}_{evap}}{\dot{Q}_{in}}=\frac{\dot{W}_T-\dot{W}_P-\dot{W}_{C1}-\dot{W}_{C2}+\dot{Q}_{evap}}{\dot{Q}_B} \quad (6)$$

Here, $\dot{Q}_B$, $\dot{Q}_{evap}$, and $\dot{W}_{net}$ denote the thermal energy rate entered into the cycle, the refrigeration rate produced in the evaporator, and the net work output of the cycle, respectively. The net work is calculated by subtracting the total power generated in the turbine from the power consumption by the pump and compressors. The exergy efficiency of the cycle can be expressed as:

$$\eta_{ex}=\frac{\dot{E}x_{out}}{\dot{E}x_{in}}=\left(1-\frac{\dot{E}x_{des,total}}{\dot{E}x_{in}}\right) \quad (7)$$

Here, $\dot{E}x_{in}$ is the total exergy input to the cycle. This is calculated by summation of the total exergy input into the cycle by the vapor generator and the total exergy entered into the cycle by the pump and the compressors. In fact, the difference between the first and second laws of thermodynamics is that the first law of thermodynamic components, such as pumps and compressors in the thermal cycles, are considered as energy consumers, while from the viewpoint of the second law of thermodynamics, these components are the entry points of the exergy into the cycle. So, the exergy efficiency of the cogeneration Rankine power and two-stage compression refrigeration cycle is calculated by the following equation:

$$\eta_{ex}=1-\frac{\dot{I}_{total}}{\dot{E}x_{input}+\dot{W}_p+\dot{W}_{C1}+\dot{W}_{C2}} \quad (8)$$

Here, $\dot{I}_{total}$ refers to the sum of exergy destruction of the cycle components that is obtained using the equations given in Table 1.

4.Ejector simulation

The ejector is the key component in the cogeneration Rankine power and two-stage compression refrigeration cycles. So far, different models have been provided to simulate the ejector. In this study, the constant-pressure mixing model is used for simulating the ejector performance due to the better and more accurate prediction of this model. The basic principle of this model was presented by Keenan et al. [24] based on gas dynamics. Then the research of Huang et al. [23] developed and generalized this principle [14]. The ejector simulation algorithm presented in this study is inspired by the Sarkar algorithm [26]. According to Fig. 2, for the given primary and secondary thermodynamic properties of the ejector and by applying the conservation of energy and momentum equations for different processes in the ejector, the output thermodynamic properties of the ejector can be calculated.

Considering the isentropic efficiency of the nozzle and applying the energy conservation to the ejector's primary nozzle, the enthalpy and velocity of the flow can be calculated.

$$\eta_n = \frac{h_3 - h_{3b}}{h_3 - h_{3b,s}} \tag{9}$$

$$h_3 = \frac{1}{2}u_{3b}^2 + h_{3b} \tag{10}$$

Based on Assumption (7), the velocity of the secondary flow after the suction is negligible. Therefore, the enthalpy of the secondary flow before and after the suction is equal, and the mixing process is done on the suction pressure, which means the ejector pressure is equal to the suction pressure. So, the conservation of momentum for the mixing process can be expressed as follows:

$$\dot{m}_3 u_{3b} = (\dot{m}_3 + \dot{m}_9)u_{m,s} \tag{11}$$

The mixing efficiency is:

$$\eta_m = \frac{u_m^2}{u_{m,s}^2} \tag{12}$$

By knowing the velocity of the flow after the mixing process, the energy-conservation equation for the mixing section can be written as:

$$\dot{m}_3\left(\frac{u_{3b}^2}{2} + h_{3b}\right) + \dot{m}_9 h_9 = (\dot{m}_3 + \dot{m}_9)\left(\frac{u_m^2}{2} + h_m\right) \tag{13}$$

Finally, at the diffuser outlet, it can be expressed as:

$$\eta_d = \frac{h_{4,s} - h_m}{h_4 - h_m} \tag{14}$$

$$h_4 = \frac{1}{2}u_m^2 + h_m \tag{15}$$

One of the key parameters for the design and simulation of the ejector is the entrainment ratio. The ejector entrainment ratio is defined as the mass flow ratio of the secondary flow to the primary flow and is given by:

$$\mu = \frac{\dot{m}_9}{\dot{m}_3} \tag{16}$$

Thus, according to the definition of the ejector entrainment ratio, Eq.(11), by using the isentropic efficiency of the mixing process, and Eq. (13) are rewritten as follows:

$$\frac{\sqrt{\eta_m}.u_{3b}}{1+\mu} \tag{17}$$

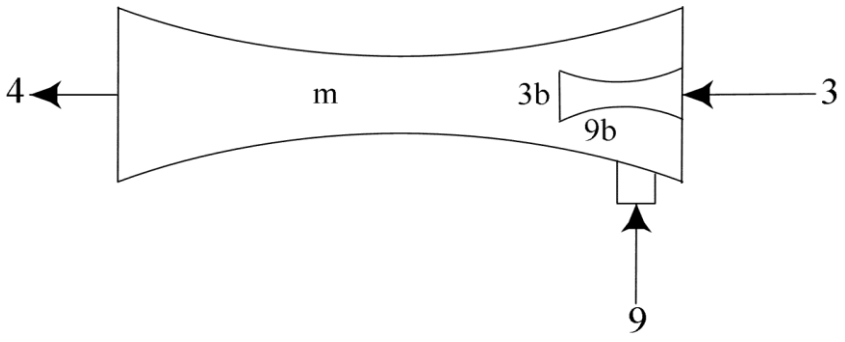

Fig 2. Schematic of the structure and processes in the ejector

$$h_m = \frac{h_3 + \mu . h_9}{1 + \mu} - \frac{u_m^2}{2} \quad (18)$$

5.Simulation algorithm and validation

A calculating program is written in EES. The simulation procedure for the energy and exergy analysis of the cycle is as follows: First, Eqs. 5 to 8 are solved, followed by the equations in Table 1. The thermodynamic analysis of the cycle is performed in the EES code format. The input information required in the simulation of the cycle is such that the equations are solved explicitly without the need for trial and error.

But in the ejector modeling, the simulation procedures will be slightly different. Due to the equations given in the ejector simulation section, there are two approaches to simulating the ejector. The first approach is when the entrainment ratio is given. Here, the equations are solved explicitly. The second approach is when the goal is to reach a given pressure in the output of the ejector. In this case, the equations are solved by trial and error with an initial value guess for the entrainment ratio to reach the required outlet pressure. Since the saturation temperature of the condenser is constant based on Assumption (2), the pressure of the ejector outlet stream must be equal to the saturation pressure corresponding to the saturation temperature of the condenser, so that the evaporator back flow does not occur. Therefore, in this study, the second approach is used. Fig. 3 shows the calculation flowchart used to solve the simulation algorithm proposed for the cogeneration cycle.

To ensure the integrity of the software code written in EES and the accuracy of the calculation results obtained from the simulation outlet by EES, first a basic code is written to simulate the Rankine power and ejector refrigeration cycle. Next, the results of the simulation of this cycle are validated by comparing this with the results of Dai et al. [14]. The comparison results for the turbine power, refrigeration output, and exergy efficiency are shown in Fig. 4. The results of the simulation match the results of Dai et al. not only qualitatively [14] but also in numerical terms. The minor differences in the results can be due to rounding-off errors in the computing process software. There may also be slight differences in the resources and database used to calculate the properties of the refrigerants in the different software programs.

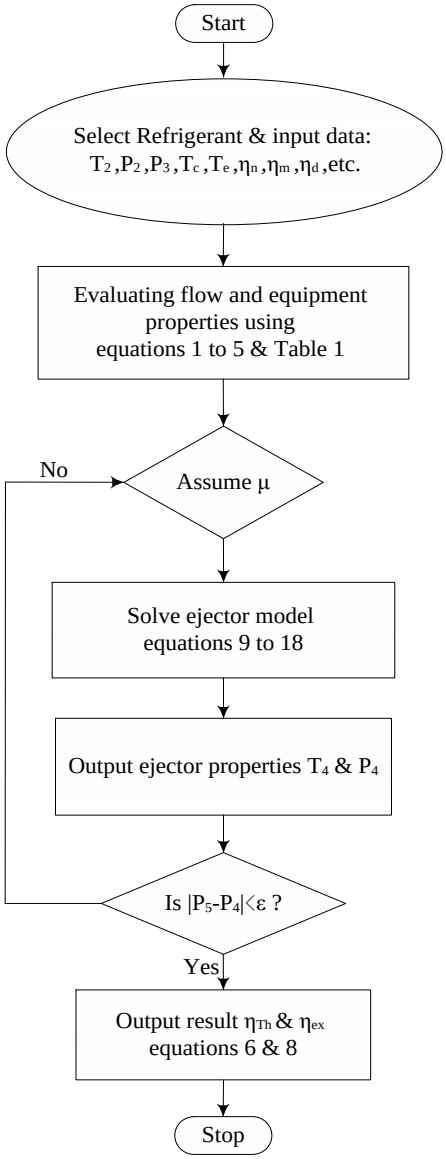

Fig 3. A simulation flowchart of the cycle analysis

6.Results and discussion

Table 3 shows the results of the energy and exergy analysis of the cogeneration organic Rankine power and two-stage compression refrigeration cycle. In the simulation for a better analysis and understanding of the cycle performance, the input data and main assumptions of the cycle are taken to be the same as in the reference [14]. This allows comparing the results of the cogeneration Rankine power and two-stage compression refrigeration cycle with the results of the conventional combined power and ejector refrigeration cycle. Some assumptions of the parameters are made as listed in Table 2. In the power section and two-stage compression refrigeration section of the cycle refrigerant, R123 and R134a are used respectively.

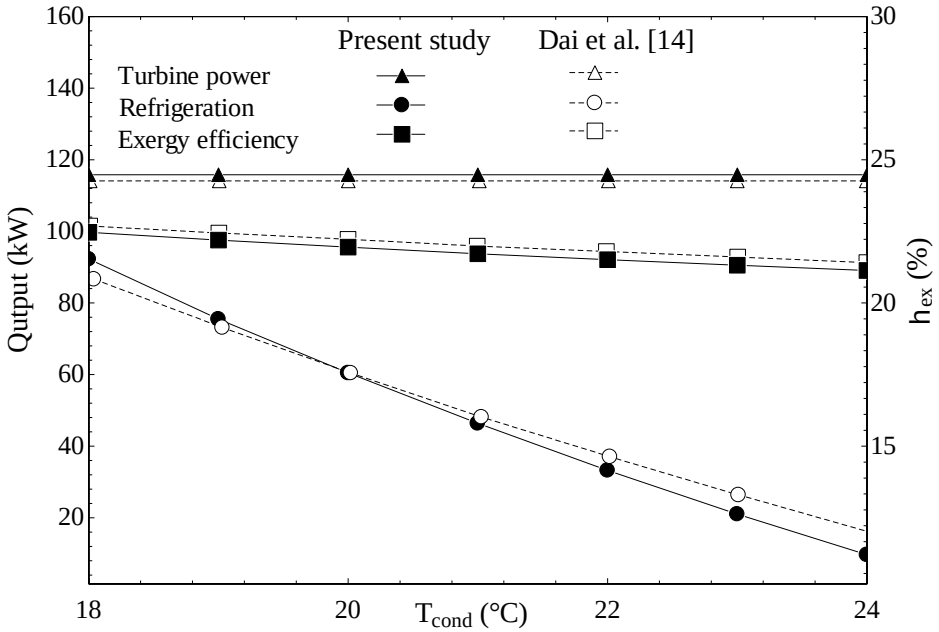

Fig 4. Validation the results of the turbine power, refrigeration output and exergy efficiency versus condenser temperature

Table 2 Main assumptions for the combined cycle

Parameter	**Value**
Heat source initial temperature (ºC)	150
Cascade condenser temperature (ºC)	-10
Evaporator temperature (ºC)	-30
Turbine inlet pressure (kPa)	800
Turbine inlet temperature (ºC)	140
Turbine back pressure (kPa)	200
Turbine isentropic efficiency (%)	0.85
Pump isentropic efficiency (%)	0.7
Nozzle efficiency of ejector (%)	0.9
Mixing efficiency of ejector (%)	0.85
Diffuser efficiency of ejector (%)	0.85
Turbine mas flow rate (kg/s)	4.921
Evaporator mas flow rate(kg/s)	1.5

Table 3 The results of energy and exergy analysis of the combined cycle

Result	**Present study**	**Dai et al. [14]**
Turbine work (kW)	115.8	114.14
Pump work (kW)	3.45	3.45
Compressor 1 work (kW)	38.01	-
Compressor 2 work (kW)	34.1	-
Refrigeration output (kW)	280.5	60.44
Net power output (kW)	40.24	110.69
Net power and refrigeration output (kW)	320.74	171.13
Thermal efficiency (%)	25.39	13.72
Exergy efficiency (%)	39.09	22.02

As shown in Table 2, the net work output of the Rankine power and two-stage compression refrigeration cycle is less than the conventional combined power and ejector refrigeration cycle due to the lack of a compressor in the conventional cycle. Large increases are seen in the refrigeration capacity of the novel cycle, and a significant increase is observed in the thermal efficiency and exergy efficiency compared to the conventional cycle. Since the increased refrigeration capacity is much higher than the decreased net power output, the thermal efficiency has increased. The increase in the exergy efficiency is due to increases in the net refrigeration exergy output of the cycle and reduction of the exergy destruction by the generator due to lack of a chimney in the generator owing to the use of solar energy.

As a key component of the cycle, it is essential to investigate the effect of the ejector entrainment ratio on the thermal and exergy efficiency. To do this, by changing the temperature of the ejector's secondary flow, the ejector entrainment ratio can be changed. By increasing the temperature of the secondary flow, which is in fact the temperature of the cascade condenser, the secondary flow rate will increase; thus, with an increase in the secondary flow pressure, the entrainment ratio increases. Figs. 5 and 6 illustrate the effect of the variations of the entrainment ratio on the thermal and exergy efficiency at various turbine inlet pressures. The variation of the secondary flow temperature of the ejector is between −15°C to 5°C.

By increasing the turbine inlet pressure, the enthalpy of the fluid increases and therefore the turbine power output increases. This causes an increase in the thermal efficiency of the cycle. But by increasing the entrainment ratio in all the turbine inlet pressures, a reduction in the thermal efficiency can be seen. The reason for the decrease of the thermal efficiency is that it increases the Compressor 1 work and the cycle refrigeration capacity decreases as μ increases.

Figure 6 shows that the exergy efficiency increases as the turbine inlet pressure decreases. This behavior can be explained with arguments similar to those presented for thermal efficiency. Also, it can be seen that the exergy efficiency increases first to a maximum value and then decreases as the entrainment ratio increases. By increasing the entrainment ratio, the ejector secondary mass flow rate increases. Increasing the secondary mass flow rate will increase the capacity of the cascade condenser, which causes a reduction of the power consumption and the exergy destruction of the high-pressure compressor. Therefore, at first, the exergy efficiency increases. But, on the other side, increasing the secondary mass flow rate increases the exergy destruction by the cascade condenser. Also, by increasing the operating temperature of the cascade condenser, the power consumption and the exergy destruction of the high-pressure compressor gradually increases. It is such that after a specific entrainment ratio, increasing the total exergy destruction has a predominant

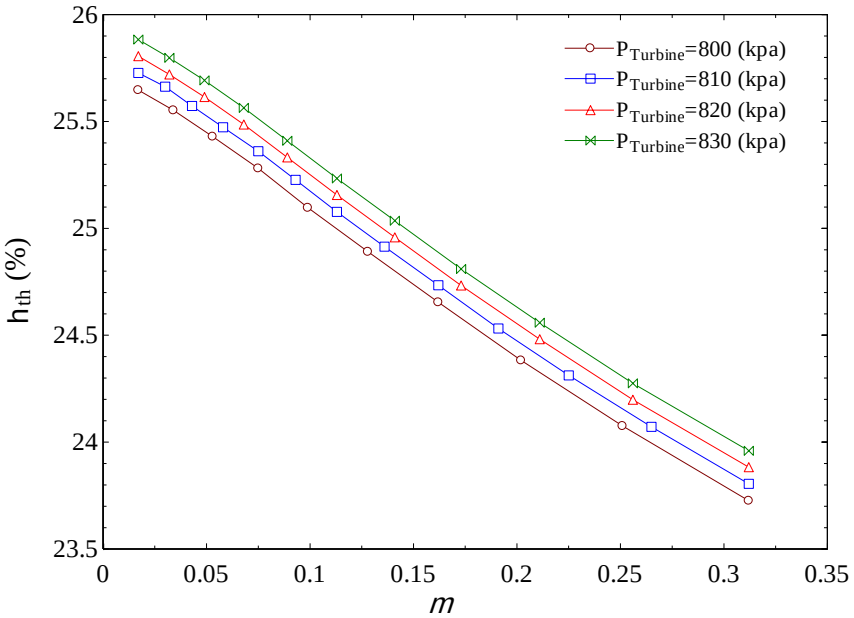

Fig 5. Effect of the entrainment ratio on the thermal efficiency at various turbine inlet pressure

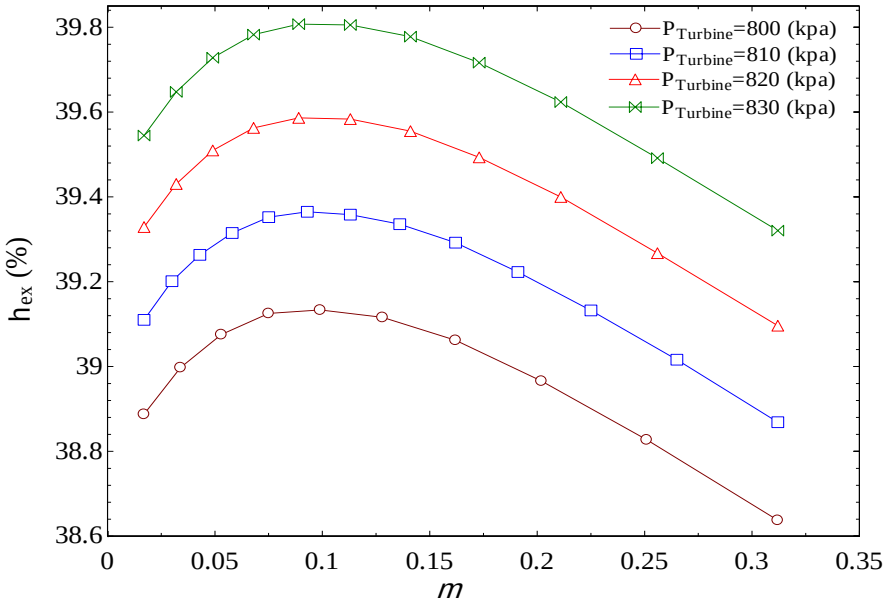

Fig 6. Effect of the entrainment ratio on the exergy efficiency at various turbine inlet pressure

effect on reducing the total exergy destruction since then the exergy efficiency decreases.

Figures 7 and 8 show the effect of variations of the evaporator temperature on the thermal and exergy efficiency at various entrainment ratios. Since in practical applications, the ejector refrigeration cycle cannot be used to produce refrigeration at very low temperatures, the ejector secondary flow temperature variations correspond to the considered entrainment ratio changes between −2°C to 5°C. As seen in Fig. 6, for an entrainment ratio more than 0.1, which approximately equates to a −5°C temperature for the ejector secondary flow, the exergy efficiency reduces as μ increases. Also, in Fig. 5, it is observed that by increasing the entrainment ratio the thermal efficiency decreases. This trend is also evident in Figs. 7 and 8.

As shown in Figs. 7 and 8, generally by increasing the entrainment ratio, the thermal and exergy efficiency decreases. But with the increase of the evaporator temperature due to the reduction in the pressure ratio of Compressor 1, the power consumption of this compressor reduces significantly. In addition, by increasing the evaporator temperature, the refrigeration capacity increases. So, in general, the thermal efficiency of the cycle increases as the evaporator temperature increases.

In the cogeneration organic Rankine power and two-stage compression refrigeration cycle, the evaporator temperature has a more important effect on the exergy efficiency. While the evaporator temperature increases, the low-pressure compressor power consumption and exergy destruction decrease.But this decline in the power consumption of the low-pressure compressor decreases the net exergy input into the cycle. Also, increasing of the evaporator temperature despite be increased the refrigeration capacity, the quality of refrigeration output of the cycle yields because of the increasing the refrigeration temperature and approaching to the ambient temperature. However, as shown in Fig. 8, at the beginning of increasing the evaporator temperature, the reduction in the exergy destruction by the low-pressure compressor has a dominant influence in the exergy efficiency; so, at first, the exergy efficiency increases. But gradually with a further increase in the evaporator temperature, the effect of decreases in the net exergy input into the cycle and the yield of the quality of refrigeration have a dominant effect on the exergy efficiency. Since then, there appears to be a decline in the exergy efficiency.

Figure 9 illustrates the effect of the evaporator temperature on the exergy efficiency in comparison with the thermal efficiency at various heat source initial temperatures. The exergy efficiency behavior can be explained qualitatively with arguments similar to those presented for Fig. 8. As shown in Fig. 9, the thermal efficiency does not change with a variation of the heat source's initial temperature and only one

graph is proposed for it. The reason for this behavior is because of the thermal efficiency only Influenced by the heat flux input to the cycle and production of the net power and refrigeration. So, as long as the inlet heat flux input to the cycle through the generator is fixed, the thermal efficiency remains constant. This behavior shows the weakness of the first law of thermodynamics

in dealing with the thermal cycle. The exergy efficiency decreases as the heat source's initial temperature increases. An increase in the inlet temperature of Therminol 66 in the generator while the outlet temperature is fixed causes an increase in the generator temperature difference; therefore, the exergy destruction of the generator increases and the exergy efficiency decreases.

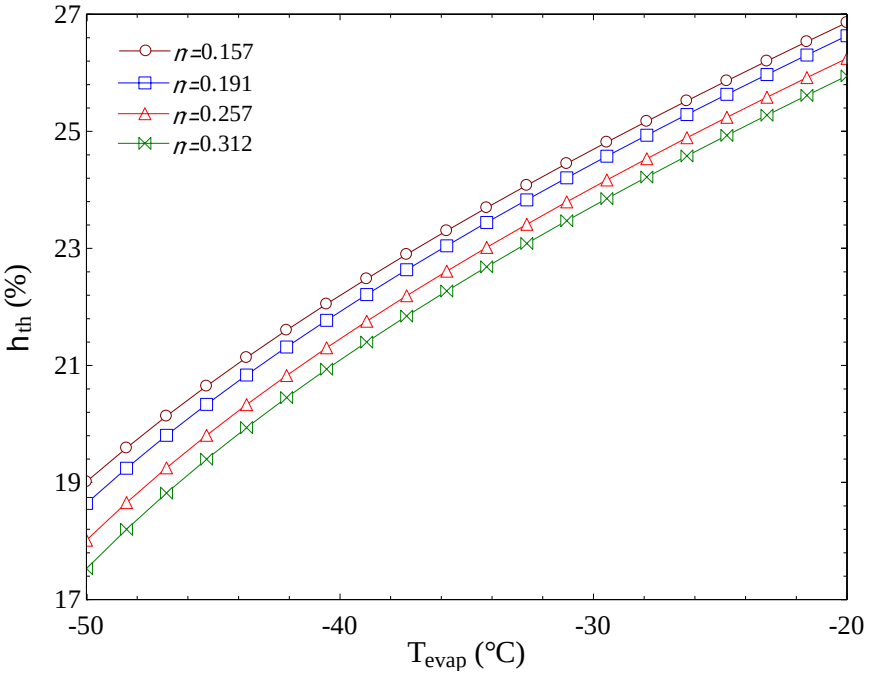

Fig 7. Effect of the evaporator temperature on the thermal efficiency at various entrainment ratio

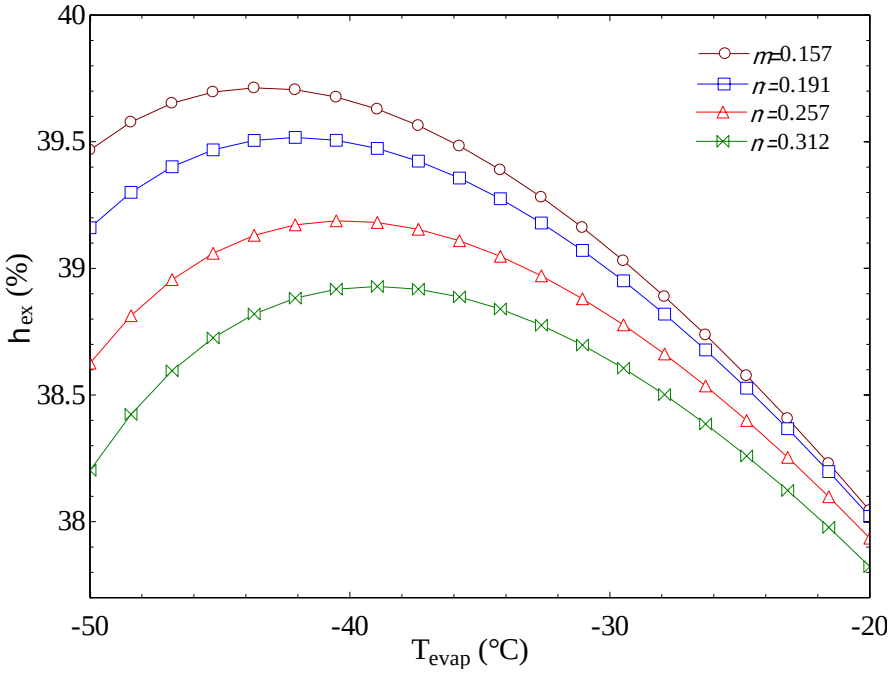

Fig 8. Effect of the evaporator temperature on the exergy efficiency at various entrainment ratio

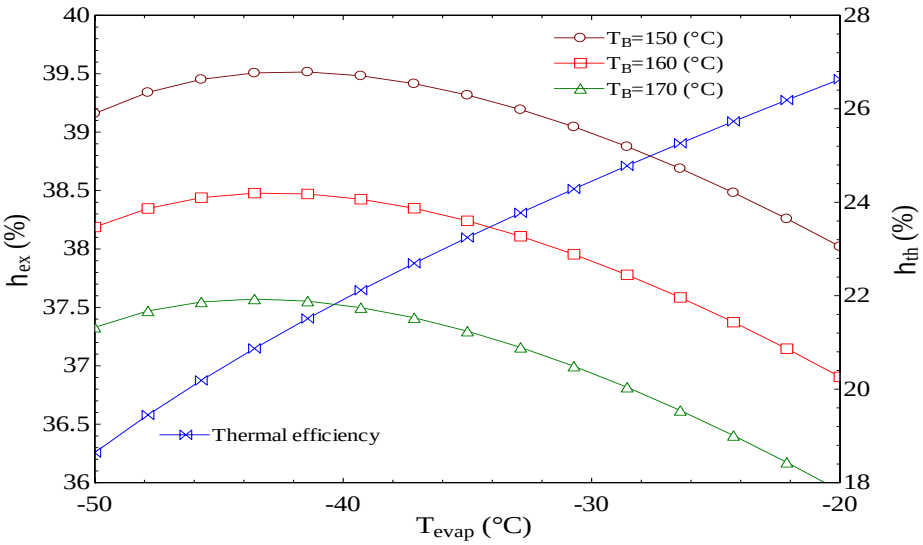

Fig 9. Effect of the evaporator temperature on the exergy efficiency in comparison with the thermal efficiency at various heat source initial temperature

7.Conclusion

The energy and exergy analysis of a novel cogeneration organic Rankine power and two-stage compression refrigeration cycle was conducted by using EES software. The results showed that the new cycle in the basic operation mode has 11.67 percent improvement in the thermal efficiency and 16.89 percent improvement in the exergy efficiency compared to the conventional combined power and ejector refrigeration cycle.

As observed in the results, because of the existence many components in the cycle, the exergy efficiency is more influenced by the variations of some parameters, such as the heat source's initial temperature and the turbine inlet pressure, and less influenced by the variations of some other parameters, such as the evaporator temperature and the cascade condenser temperature. Even though the net work output of the cycle is reduced, a significant increase occurs in the refrigeration capacity of the cycle. The advantages of using this new cogeneration organic Rankine power and two-stage compression refrigeration cycle includes the higher thermal efficiency, the higher exergy efficiency, and increased access to more refrigeration capacity at the lower temperature compared to the conventional combined power and ejector refrigeration cycle. In the conventional ejector refrigeration cycle, refrigeration cannot be achieved at very low cooling temperatures. The main idea of presenting this new cycle is based on higher refrigeration production at lower temperatures. Since this cycle has substantially improved the thermal and exergy efficiency, it is recommended to use this instead of the conventional combined power and ejector refrigeration cycle.

References

[1] Zhang Zh., Wang H., Tian L., Huang Ch., Thermodynamic Analysis of Double-Compression Flash Intercooling Transcritical CO2 Refrigeration Cycle, The Journal of Supercritical Fluids (2016)109: 100-108.

[2] Li H., Cao F., Bu X., Wang L., Wang X., Performance Characteristics of R1234yf Ejector-Expansion Refrigeration Cycle, Applied Energy (2014)121: 96-103.

[3] Wang F., Li D.Y., Zhou Y., Analysis for the Ejector Used as Expansion Valve in Vapor Compression Refrigeration Cycle, Applied Thermal Engineering (2016) 96: 576-582.

[4] Lawrence N., Elbel S., Theoretical and Practical Comparison of Two-Phase Ejector Refrigeration Cycles Including First and Second Law analysis, International Journal of Refrigeration (2013)36: 1220-1232.

[5] Zhang Zh., Tong L., Chang L., Chen Y., Wang X., Energetic and Exergetic Analysis of an Ejector-Expansion Refrigeration Cycle Using the Working Fluid R32, Entropy (2015) 17: 4744-4761.

[6] Elgendy E., Parametric Study of a Vapor Compression Refrigeration Cycle Using a

Two-Phase Constant Area Ejector, International Journal of Mechanical, Aerospace, Industrial, Mechatronic and Manufacturing Engineering (2013) 7.
[7] Xing M., Yan G., Yu J., Performance Evaluation of an Ejector Subcooled Vapor-Compression Refrigeration Cycle, Energy Conversion and Management, (2015)92: 431-436.
[8] Wang X., Yu J., Zhou M., Lv X., Comparative Studies of Ejector-Expansion Vapor Compression Refrigeration Cycles for Applications in Domestic Refrigerator-Freezers, Energy, (2014)70: 635-642.
[9] Zhu Y., Jiang P., Hybrid Vapor Compression Refrigeration System with an Integrated Ejector Cooling Cycle, Applied Energy (2012) 35: 68-78.
[10] Chen J., Havtun H., Palm B., Parametric Analysis of Ejector Working Characteristics in the Refrigeration System, Applied Thermal Engineering (2014)69: 130–142.
[11] Sorouradin A., Saberi A., Mahmoudi S.M., Development of New Model to Prediction the Performance of Ejector Refrigeration Cycle, Modares Mechanical Engineering (2012)12: 133-146.
[12] Adrian G., Dobrovicescu A., Grosu L., Cerna E., Energy and Exergy Analysis of an Ejector Refrigeration System, U.P.B. Sci. Bull (2013)75.
[13] Lontsi F., Hamandjoda O., Mayi O.T., Kemajou A., Development and Performance Analysis of a Multi-Temperature Combined Compression/Ejection Refrigeration Cycle Using Environment Friendly Refrigerants, International Journal of Refrigeration (2016)69: 42-50.
[14] Dai Y., Wang J., Gao L., Exergy Analysis, Parametric Analysis and Optimization for a Novel Combined Power and Ejector Refrigeration Cycle, Applied Thermal Engineering (2005) 29:1983-1990,.
[15] Zheng B., Weng Y.W., A Combined Power and Ejector Refrigeration Cycle for Low Temperature Heat Source, Solar Energy (2010) 84: 784-791.
[16] Habibzadeh A., Rashidi M.M., Galanis N., Analysis of a Combined Power and Ejector Refrigeration Cycle Using Low Temperature Heat, Energy Conversion and Management (2013) 65: 381-391.
[17] Wang J., Dai Y., Sun Zh., A Theoretical Study on a Novel Combined Power and Ejector Refrigeration Cycle, International Journal of Refrigeration (2009)32: 1186-1194.
[18] Kim, K., Han Ch., Kim S., Ko H., Performance Analysis of a Combined Power and Ejector Refrigeration Cycle for Different Working Fluids ", International Journal of Mining, Metallurgy & Mechanical Engineering (2013) 1.
[19] Yang X., Zhao L., Li H., Yu Zh., Theoretical Analysis of a Combined Power and Ejector Refrigeration Cycle Using Zeotropic Mixture, Applied Energy (2015) 160: 912-919.
[20] Yang X., Zhao L., Thermodynamic Analysis of a Combined Power and Ejector Refrigeration Cycle Using Zeotropic Mixtures, Energy Procedia (2015) 75: 1033-1036.
[21] Yang X., Zheng N., Zhao L., Deng Sh., Li H., Yu Zh., Analysis of a Novel Combined Power and Ejector-Refrigeration Cycle, Energy Conversion and Management (2016) 108: 266-274.
[22] Dincer I., Rosen M. A., Exergy, Energy, Environment and Sustainable Development, Elsevier (2007).
[23] Brunin O., Feidt M., Hivet B., Comparison of the Working Domains of Some Compression Heat Pumps and a Compression-Absorption Heat Pump, International Journal of Refrigeration (1997)20: 308-318.
[24] Keenan H., Neumann E.P., Lustwerk F., An Investigation of Ejector Design by Analysis and Experiment, Journal of Applied Mechanics Transactions of the ASME (1950)72: 299-309.
[25] Huang B.J., Chang J.M., Wang C.P., Petrenko V.A., A 1-D Analysis of Ejector Performance, International Journal of Refrigeration (1999) 22: 354-364.
[26] Sarkar J., Performance Characteristics of Natural-Refrigerants Based Ejector Expansion Refrigeration Cycles, Journal of Power and Energy (2009)223: 543-550.